Journal of Engineering Mathematics **32:** 343–364, 1997.

Coupled double-diffusive thermocapillary instability: Linear and nonlinear analysis

LEONID BRAVERMAN[1,2] and ALEXANDER ORON[1]
[1]*Department of Mechanical Engineering, Technion-Israel Institute of Technology, Haifa 32000, Israel*
[2]*Department of Computers, International College ORT Braude, Carmiel 20101, Israel*

Received 2 January 1996; accepted 28 November 1996

Abstract. The onset of Marangoni instability of the quiescent equilibrium in a binary liquid layer open to the atmosphere at its nondeformable interface in the no-gravity environment and subjected to the simultaneous presence of the normal temperature gradient and of the tangential temperature and solute concentration gradients is studied. The no-flow equilibrium is possible for specially chosen values of the imposed tangential gradients only. Linear stability analysis shows that the instability is longwave for very small values of the parameter γ that specifies the ratio between the tangential and normal temperature gradients. For higher values of γ the instability is shortwave. It is found in the latter case that the instability is always oscillatory for nonzero γ and for any value of the inverse Lewis number $L^{-1} \neq 1$. Weakly nonlinear analysis in the regime of small γ is carried out to derive the nonlinear evolution equation describing a wave propagation along the layer. The primary bifurcation from the equilibrium state is found to be supercritical for *very small* values of γ and becomes subcritical thereafter.

Key words: Marangoni, double-diffusion, zero gravity, nonlinear.

1. Introduction

There is a significant amount of research done on Marangoni instability in a pure fluid layer [1]. However, relatively little research exists on the Marangoni instability in a layer of a liquid binary mixture. It was found in experiments that surface tension acting at the free surface depends on both temperature and solute concentration. In a majority of mixtures surface tension decreases with temperature and increases (decreases) with concentration of an inorganic (organic) solute. Therefore, if a layer of a binary mixture is subjected to both temperature and concentration gradients, nonuniformities of those at the free surface lead to the emergence of surface shear stresses that are able under certain conditions to destabilize the ground equilibrium state.

It is now well known that the simultaneous presence of two or more components with different diffusivities in a liquid layer may lead to a variety of new phenomena. The case of a liquid layer heated from above, which is stable under regular conditions (stable stratification) can be given as an example. It may lose its stability if a destabilizing concentration gradient is imposed along with the heating [2]. A layer subjected to a stabilizing solute concentration can exhibit an oscillatory instability when a destabilizing thermal gradient across it is opposed to the former [3]. This oscillatory instability was tested experimentally in [4] and some discrepancies between the theory and the experiments were found. Diffusion, which generally serves as a stabilizing agent, may give rise to what is called thermosolutal instability. This kind of phenomenon is frequently called a double-diffusive phenomenon if two or more components with different diffusivities are present in a fluid and their gradients make opposing contributions as a possible source of instability. An extensive review of the work on double-

diffusive phenomena related mainly to buoyancy-induced effects and their applications in oceanography, chemistry, metallurgy, geology, geophysics, etc., is found in [5, 6].

Various transport processes encountered in technology and nature are owing to or affected by simultaneous action of temperature and solute concentration gradients. Different configurations of those gradients have been delineated in [7] in the context of buoyancy-driven convection. Similar configurations can also be considered in the context of surface-tension-driven convection in the no-gravity environment. Relevant examples are different techniques of materials processing, *e.g*. crystal growth, from binary or multicomponent liquid mixtures. Many of them, especially those employing the floating-zone and temperature-gradient methods, involve large temperature and possibly concentration gradients imposed in various directions relative to the melt [7].

To the best of our knowledge the literature is not abundant with research on double-diffusive effects in the context of interfacial phenomena. Linear stability analysis of the quiescent equilibrium in a layer with a free surface under the action of *normal* temperature and concentration gradients in a zero-gravity environment was done in [8]. It was found that, when both the thermal and solutal Marangoni numbers are positive, *i.e*. the shear stresses induced separately by thermal and concentration components enhance each other, the motionless state can lose its stability monotonically. However, when the Marangoni numbers have opposite signs, *i.e*. when the shear stresses induced separately by thermal and solutal components counteract, the instability is mostly oscillatory. The results of [8] were completed and extended in [9]. The existence of a double-zero singularity point (or a codimension-2 point), *i.e*. a point in the space of parameters where stationary and oscillatory instabilities compete, was demonstrated. Nonlinear analysis in the neighborhood of the double-zero point revealed that the finite amplitude steady rolls suppress the oscillatory rolls.

Numerical study of double-diffusive Marangoni convection in a binary fluid contained in a two-dimensional cavity simultaneously subjected to tangential temperature and solute concentration gradients was done in [10]. The main result was that convection may occur, even when the overall Marangoni number vanishes, *i.e*. when the shear stresses arising separately from the temperature and concentration nonuniformities are equal at equilibrium. Convection occurs owing to the difference in the characteristic 'thermal' and 'diffusive' times related, respectively, to the thermal diffusivity of the fluid and the mass diffusivity of the solute in the solvent. However, the onset of such a convection as arising from instability of the no-flow equilibrium has not yet been investigated.

It is the purpose of the present work to study the instability of a binary liquid layer open to the atmosphere and subjected simultaneously to the normal temperature gradient and both small tangential temperature and solute concentration gradients. Similar to the assumptions made in [11], the interfacial deformation is neglected. The problem considered in [10] is thus a particular case of the more general situation addressed here. We refer to the instability arising from this configuration as to coupled double-diffusive thermocapillary instability. It is found that, if the appropriate Biot number of the system vanishes, the type of this instability (longwave or shortwave) is determined by the value of the parameter γ specifying the ratio between the tangential and normal temperature gradients: for small γ the instability is longwave, while for larger ones it is shortwave when the Biot number of the system is zero. It is shown that the instability is always oscillatory when the inverse Lewis number L^{-1} of the binary liquid is different from unity. Using the approach of asymptotic expansions, we derive the nonlinear evolution equation describing the spatio-temporal behavior of the flow, temperature and concentration fields. The perturbations are found to grow, saturate in the

amplitude and propagate along the layer in the direction depending uniquely on the sign of $\gamma(L^{-1}-1)$.

The paper is organized as follows. In Section 2 we formulate the problem and the governing equations. Section 3 is devoted to the linear stability analysis of the quiescent equilibrium state. In Section 4 the weakly nonlinear analysis is carried out to derive the evolution equation describing the behavior of the system slightly beyond the onset of instability. Section 5 contains a study of some properties of the traveling-wave patterns emerging in the system under consideration. In Section 6 we report the results of a numerical study of the evolution equation derived in Section 4. Section 7 summarizes the results of the paper.

2. Statement of the problem and governing equations

The basic set-up studied in this work is similar to that outlined in [10]. A binary liquid mixture is held in a vessel of a large aspect ratio open to the ambient gas phase. The rigid bottom and the free surface of the mixture are impermeable for the solute and a temperature gradient is imposed across the system. The vertical walls of the container are kept at fixed and different temperatures and solute concentrations. These prescribe tangential gradients of the corresponding fields.

An idealized configuration adopted for our study is now described. We consider a layer of an incompressible binary fluid of infinite extent in the tangential directions x and y and thickness h lying on a rigid plane and exposed to the ambient gas phase at its nondeformable (due to large surface tension or large aspect ratio of the layer) free surface. The layer is subjected to a normal temperature gradient, $\{0,0,-a\}, a>0$. Note that heating from below (above) corresponds to $a>0$ ($a<0$). In addition, two tangential uniform gradients are imposed: a temperature gradient and a concentration gradient. The surface tension σ is assumed to be dependent upon both temperature T and solute concentration $C, \sigma=\sigma(T,C)$, and therefore thermo- and soluto-capillary effects are taken into accout.

We now proceed to the formulation of the mathematical model used below. A set of governing equations in the absence of gravity and of cross-effects, such as the Soret (mass transport resulting from thermal gradients) and Dufour (heat transfer owing to species gradients) effects, is given by

$$\begin{aligned} &\nabla\cdot\mathbf{v}=0, \qquad \frac{\partial\mathbf{v}}{\partial t}+(\mathbf{v}\nabla)\mathbf{v}=-\frac{1}{\rho}\nabla p+\nu\nabla^2\mathbf{v}, \\ &\frac{\partial T}{\partial t}+\mathbf{v}\nabla T=\chi\nabla^2 T, \qquad \frac{\partial C}{\partial t}+\mathbf{v}\nabla C=D\nabla^2 C. \end{aligned} \tag{1}$$

Here $\mathbf{v}, T, p, C,$ are, respectively, fields of the fluid velocity, temperature, pressure and solute concentration, ν, χ, D are, respectively, kinematic viscosity, thermal diffusivity and mass diffusivity of the mixture, ρ is its reference density and t is time. It should be clear that the problem formulated here is (and has to be) considered in the *no-gravity* environment. If in the presence of gravity the heating is perpendicular to the direction of the gravity force, equilibrium is impossible due to natural convection. This is in contrast with the case of a heating parallel to the gravity force, *i.e.* from below, in which the buoyancy-driven convection can be, in the case of shallow layers, neglected with respect to the surface-tension driven one.

The boundary conditions at the rigid bottom surface are the no-flow condition for the velocities, a specified heat flux and mass impermeability, respectively.

$$\mathbf{v} = 0, \qquad \frac{\partial T}{\partial z} = -a, \qquad \frac{\partial C}{\partial z} = 0, \quad \text{at } z = 0. \tag{2}$$

At the free surface the boundary conditions are, respectively, the kinematic boundary condition, heat transfer governed by Newton's law of cooling and mass impermeability

$$v_z = 0, \qquad \kappa \frac{\partial T}{\partial z} + q(T - T_\infty) = 0, \qquad \frac{\partial C}{\partial z} = 0, \quad \text{at } z = h, \tag{3}$$

where κ is the thermal conductivity of the mixture, q is the rate of heat transfer by convection at the free surface at T_∞ is the imposed temperature of the ambient gas phase. Also, the balance of tangential stresses at the free surface is given by

$$\mu \frac{\partial v_x}{\partial z} = \frac{\partial \sigma}{\partial x}, \qquad \mu \frac{\partial v_y}{\partial z} = \frac{\partial \sigma}{\partial y} \tag{4}$$

and under the assumption of linear dependence of surface tension σ on both temperature and concentration we have

$$\sigma(T, C) = \sigma_0 - \sigma_t(T - T_r) + \sigma_c(C - C_r).$$

Equations (4) are rewritten in the form

$$\mu \frac{\partial v_x}{\partial z} = -\sigma_t \frac{\partial T}{\partial x} + \sigma_c \frac{\partial C}{\partial x}, \qquad \mu \frac{\partial v_y}{\partial z} = -\sigma_t \frac{\partial T}{\partial y} + \sigma_c \frac{\partial C}{\partial y} \quad \text{at } z = h, \tag{5}$$

wherein $\sigma_t = -\partial\sigma/\partial T, \sigma_c = \partial\sigma/\partial C, \mu = \nu\rho$ is the fluid viscosity, and T_r and C_r are the reference temperature and concentration, respectively. For most aqueous solutions of inorganic salts surface tension decreases with temperature and increases with salt concentration, hence the values of σ_t and σ_c are positive for that choice of a mixture. For aqueous solutions of organic solutes surface tension usually decreases with concentration, and therefore in that case σ_c will be negative.

3. Linear stability analysis of the equilibrium

We first investigate linear stability properties of the equilibrium of a two-dimensional layer given by

$$\mathbf{v}_0 = 0, \qquad T_0(x, z) = T_r + Ax - az, \qquad C_0(x, z) = C_r + \frac{\sigma_t}{\sigma_c} Ax \equiv C_r + A_c \cdot x, \tag{6}$$

$$T_\infty = T_r + Ax - \frac{a(\kappa + qh)}{q}.$$

Also, without loss of generality, we can assume that $A > 0$ meaning that the tangential temperature gradient is directed from the left to the right. It follows from Equation (5) that a two-dimensional no-flow equilibrium is possible only if $\sigma_t \partial T/\partial x - \sigma_c \partial C/\partial x = 0$ and

therefore the imposed tangential temperature and concentration gradients are tightly related. Note that if $A_c \neq \sigma_t A/\sigma_c$ a quiescent equilibrium is impossible and a coupled thermocapillary–soluto-capillary flow sets in under the action of the unbalanced surface shear stresses. Study of its stability is also of particular interest, however, it is outside the scope of this paper and will be discussed elsewhere.

We linearize the governing equations and the boundary conditions around the equilibrium (6) and introduce 'normal' perturbations proportional to $\exp(\lambda t)$, where λ is the complex growth rate of the perturbation. Stability properties of the equilibrium are determined by the sign of the real part of λ. The equation $\mathrm{Re}(\lambda) = 0$ defines the threshold of instability. The domain of stability (instability) corresponds to that of $\mathrm{Re}(\lambda) < 0$ ($\mathrm{Re}(\lambda) > 0$).

Scaling length, time, velocity, temperature, concentration and pressure in the units of $h, h^2/\chi, \chi/h, ah, (\sigma_t A h\chi)/(D\sigma_c)$ and $(\rho\nu\chi)/h^2$, respectively, we obtain the dimensionless form of the linearized governing equations

$$\begin{aligned} &\nabla\cdot\mathbf{v} = 0, \qquad P^{-1}\lambda\mathbf{v} = -\nabla p + \nabla^2\mathbf{v}, \\ &\lambda T + \gamma v_x - v_z = \nabla^2 T, \qquad L^{-1}\lambda C + v_x = \nabla^2 C, \end{aligned} \tag{7}$$

wherein $\mathbf{v}, T, C$ are from now on the spatial planforms of the perturbations of the velocity, temperature and concentration fields, respectively, and the subscripts denote the respective components of the velocity vector. Here $P = \nu/\chi$ is the Prandtl number and $L^{-1} = \chi/D$ is the inverse Lewis number of the mixture. The parameter $\gamma = A/a$ specifies the ratio between the tangential and the normal temperature gradients. In the case of $\gamma = 0$ the problem reduces to that of Marangoni convection in a pure liquid layer [10]. The boundary conditions are rewritten as

$$\begin{aligned} &\mathbf{v} = \frac{\partial T}{\partial z} = \frac{\partial C}{\partial z} = 0 \quad \text{at } z = 0, \\ &v_z = \frac{\partial C}{\partial z} = 0, \qquad \frac{\partial T}{\partial z} = -BT, \\ &\frac{\partial v_x}{\partial z} = -M\left(\frac{\partial T}{\partial x} - L^{-1}\gamma\frac{\partial C}{\partial x}\right), \qquad \frac{\partial v_y}{\partial z} = -M\left(\frac{\partial T}{\partial y} - L^{-1}\gamma\frac{\partial C}{\partial y}\right) \quad \text{at } z = 1. \end{aligned} \tag{8}$$

The dimensionless parameters that appear in the boundary conditions are the ('normal') Marangoni number $M = (\sigma_t a h^2)/(\mu\chi)$, and the Biot number $B = qh/\kappa$.

We consider here only 2-D perturbations of the velocity, $\mathbf{v}(x,z,t) = \{u(x,z,t), 0, v(x,z,t)\}$, temperature and concentration fields. Thus, all unknown functions are independent of y. (Although we were unable to find an appropriate Squire's transformation reducing the eigenvalue problem written for the case of 3-D perturbations $\mathbf{v}(x,y,z,t)$ to that of 2-D perturbations, we compared the values of the critical Marangoni number calculated for both cases. The main result of this comparison was that the critical value of the Marangoni number in the 3-D case is higher than the one reported below for the 2-D case independent of y. That means that the 2-D perturbations are more dangerous.) Introducing the streamfunction $\psi(x,z)$ ($v_x = \partial\psi/\partial z, v_z = -\partial\psi/\partial x$) into Equations (7, 8) and substituting normal perturbations in the form $\{\psi(x,z), T(x,z), C(x,z)\} = \{\psi^*(z), T^*(z), C^*(z)\} \times \exp(ikx)$, with

the wavenumber k in the tangential direction, x, then omitting asterisks, we obtain the linear eigenvalue problem

$$\begin{aligned} &P^{-1}\lambda(\psi'' - k^2\psi) = \psi^{(\mathrm{IV})} - 2k^2\psi'' + k^4\psi, \\ &\lambda T + \gamma\psi' + ik\psi = T'' - k^2 T, \\ &L^{-1}\lambda C + \psi' = C'' - k^2 C, \end{aligned} \tag{9}$$

with the boundary conditions

$$\psi = \psi' = T' = C' = 0 \quad \text{at } z = 0,$$

$$\psi = C' = 0, \qquad T' = -BT, \qquad \psi'' = -ikM(T - L^{-1}\gamma C) \quad \text{at } z = 1. \tag{10}$$

Here primes denote derivatives with respect to z.

Equations (9), (10) determine the spectrum of the eigenvalues λ depending on the parameters of the problem. At the transition from a stable to an unstable regime the real part of the leading eigenvalue $\bar{\lambda}$ vanishes. If $\mathrm{Im}(\bar{\lambda}) = 0$, the instability is stationary, *i.e.* time-independent, while for $\mathrm{Im}(\bar{\lambda}) \neq 0$, the instability is oscillatory, *i.e.* time-periodic. By solving Equations (9), (10) for any set of parameters P, L^{-1}, γ, we can find neutral curves, *i.e.* pairs of values M and k satisfying the condition $\mathrm{Re}(\bar{\lambda}) = 0$.

We now summarize our results related to the case of the thermally insulating free surface, $B = 0$. It is known that if this kind of thermal boundary condition is applied in the case of a pure fluid layer with strictly vertical temperature gradient, the instability is always longwave and stationary. The corresponding critical value of the Marangoni number is $M_0 = 48$ [10]. Expanding the variables of Equations (9), (10) in powers of ik for small wavenumbers k (longwave expansion)

$$\{\psi, T, C\} = \{\psi^{(0)}, T^{(0)}, C^{(0)}\} + ik\{\psi^{(1)}, T^{(1)}, C^{(1)}\} + (ik)^2\{\psi^{(2)}, T^{(2)}, C^{(2)}\} + \cdots,$$

$$M = M_0 + (ik)^2 M_2 + \cdots, \qquad \lambda = \lambda_0 + ik\lambda_1 + (ik)^2\lambda_2 + (ik)^3\lambda_3 + \cdots$$

with real λ_i and introducing these expressions into Equations (9), (10), we obtain, after equating like powers of k, a sequence of linear problems to be solved. Looking for the condition to be satisfied at the threshold of instability given by $\mathrm{Re}(\lambda) = 0$, we infer that the even components of λ should vanish, *i.e.* $\lambda_0 = \lambda_2 = \cdots = 0$.

At zeroth order of expansion we obtain $\psi^{(0)} = 0, T^{(0)} = b_0 = \text{const}, C^{(0)} = d_0 = \text{const}$. At first order of expansion the solution is given by

$$\psi^{(1)} = (d_0 - b_0)M_0(z-1)z^2/4, \qquad T^{(1)} = b_1 + \gamma(b_0 - d_0)M_0(4z^3 - 3z^4)/48,$$

$$C^{(1)} = d_1 + (b_0 - d_0)M_0(4z^3 - 3z^4)/48,$$

where b_1, d_1 are new constants of integration. This solution can be obtained only if $\lambda_1 = 0$. It should be emphasized that in the absence of a concentration gradient along the layer, $A \to 0$ ($\gamma \to 0$), $T^{(1)} = b_1 = \text{const}$ and $C^{(1)}$ is a polynomial in z in contradiction with the expected result of $C^{(1)} \to 0$. However, this apparent contradiction is due to the choice of the normalization unit for the solute concentration. That is proportional to A and therefore, when $A \to 0$, the dimensional concentration goes to zero as expected.

At second order of expansion the corresponding equations for $T^{(2)}, C^{(2)}$ can be resolved only if $d_0 = 0$ and

$$M_0 = 48, \tag{11a}$$

thus yielding the neutral Marangoni number. Also, $T^{(2)}, C^{(2)}$ are polynomials of the fifth and fourth powers in z, respectively, and $\psi_2 = 12(1-z)z^2[(b_1-d_1)+\gamma(1-L^{-1})b_0]$. At third order of expansion the equations for $T^{(3)}, C^{(3)}$ are solvable only if $\lambda_3 = 3\gamma(L^{-1}-1)/5$. Therefore, the frequency of the neutral perturbations $\omega = \mathrm{Im}(\lambda)$ at the lowest order of approximation in the longwave domain is given by

$$\omega = \tfrac{3}{5}k^3\gamma(L^{-1}-1). \tag{11b}$$

Carrying on to fourth order of expansion we find that

$$M_2 = -\tfrac{16}{25}[5 + 27\gamma^2(L^{-1}-1)^2] < 0,$$

which ensures that in the neighborhood of $k = 0$ the minimal Marangoni number is attained at $k = 0$. As will be reported below, it does not necessarily mean that the instability is always longwave. However, the longwave character of the instability survives the presence of tangential temperature and concentration gradients although the critical wavenumber may be nonzero. It thus follows from Equations (11) that the instability is oscillatory for any $\gamma \neq 0$ excluding the case of $L^{-1} = 1$.

The oscillatory nature of instability demonstrated by Equation (11b) is a result of the loss of the left–right symmetry in the system due to the existence of longitudinal temperature and concentration gradients. The specific value of the inverse Lewis number $L^{-1} = 1$ corresponds to the case of the equal relaxation times for temperature and concentration perturbations. Under these circumstances the symmetry is restored and the instability is stationary. The stationary character of instability for the case of $L^{-1} = 1$ and zero Biot number can be shown formally by writing Equations (9), (10) in terms of ψ and $H = T - \gamma C$. Equations (9), (10) are thus reduced to a set of equations equivalent to that obtained for small perturbations in the classical Pearson problem. The latter being a particular case of our problem at $\gamma = 0$ was shown [11] to have only stationary modes of instability. The balance between the relaxation times expressed by the inverse Lewis number, L^{-1}, defines the sign of the neutral oscillations frequency ω given by Equation (11b). If $L^{-1} > 1$, the heat dissipates fast and the system is affected by the concentration component of surface tension. However, if $L^{-1} < 1$ the picture is opposite, *i.e*. mass diffusion is fast, and the system is primarily driven by thermally-induced surface shear stresses. Then, the frequency ω changes its sign with respect to the previous case.

The eigenvalue problem (9), (10) was studied numerically for both finite and small values of k. We calculated the solution for Equations (9), (10), using both the 4th-order Runge–Kutta method and a method based on Chebyshev-polynomials expansions. The results obtained from the computations with these methods are in excellent agreement with each other. The calculations were carried out for the case of aqueous solution of salt. $P = 6{\cdot}7, L^{-1} = 101$. We focus first on the case of positive γ. For small k our numerical results match those of Equations (11) well. It was found that even very small tangential gradients (small γ) induce diverse kinds of instability. For $\gamma \approx 0{\cdot}0035$ the monotonic neutral curve topologically similar to that of $\gamma = 0$ undergoes a deformation and a new local minimum appears at finite

wavelengths ($k \sim 1$), while a local maximum emerges in the longwave range ($k \sim 0{\cdot}1$). A further small increase in γ results in a transformation of the local minimum to the global one, at $\gamma \approx 0{\cdot}02$, and as a result the character of instability changes from longwave to shortwave, *i.e*. of a finite wavelength. There also exists a specific value of γ at which the neutral curve has two equal minima corresponding to the critical value of $M = 48$. In this case two different modes, the thermocapillary longwave and the double-diffusive shortwave ones coexist. With a further increase of γ the local maximum rises, while the minimum descends and for $\gamma \approx 0{\cdot}055$ the neutral curve splits into two branches, one of which corresponds to a long wavelength and the other to a short one. These two branches are separated by an asymptotic line. This is summarized in Figure 1. For any nonzero value of γ at which the critical wavenumber $k_c \neq 0$ the instability is oscillatory, and the curve $\omega(k)$ also breaks into two branches for the same value of $\gamma \approx 0{\cdot}055$ as shown in Figure 2. A further increase of γ leads to a monotonic decrease of the critical value of the Marangoni number, M_c, and at the same time to an increase of the corresponding values of the frequency of the neutral oscillations ω_c and the critical wavenumber k_c. The domain of existence of the longwave branch of the neutral curve becomes narrower with increase of γ. For large values of γ an asymptotic relationship $M_c\gamma \approx 13{\cdot}5$ is found. To find an interpretation of this result let us consider the case where no normal temperature gradient is imposed while both tangential temperature and concentration gradients remain. This purely double-diffusive case corresponds to $a = 0$ which is equivalent to $\gamma = \infty$. Then, the governing Equations (1)–(4) are to be normalized with respect to the same scales as done above except for the temperature which is now scaled with respect to Ah. The new relevant, ('tangential'), Marangoni number $M^{(A)}$ is then defined as $M^{(A)} = (\sigma_t A h^2)/(\mu\chi)$. It is clear that $M^{(A)} = \gamma M$. Thus, the asymptotic relationship $M_c\gamma \approx 13{\cdot}5$ found above is equivalent to $M^{(A)} \approx 13{\cdot}5$ at the onset of instability. It is also clear that the critical value of the Marangoni number $M^{(A)}$ depends on the values of the inverse Lewis and Prandtl numbers.

Before we proceed to the case of negative γ we note that the change of the sign of γ can be achieved by changing the sign of either one A or a. It is clear that if the sign of A is changed, *i.e*. the direction of the tangential gradients imposed on the layer is reversed, the critical value of M is not affected, while the critical value of $M^{(A)}$ changes its sign. However, if the sign of a is changed, *i.e*. the direction of the vertical temperature gradient is reversed, the basic stability properties of the layer change and *no* symmetry in critical values of M is expected. Our study shows that in the case of a layer subjected only to tangential gradients ($a = 0$, *i.e*. $\gamma = \infty$) double-diffusive instability exits. Moreover, even an addition of the normal stabilizing $(a < 0)$ temperature gradient will not eliminate double-diffusive instability induced by the tangential gradients of temperature and solute concentration. This is summarized in Figure 3. It displays the critical threshold of the coupled double-diffusive instability in the space ($M^{(A)}$ vs. M). Each point of the curve represents a pair $(M, M^{(A)}) \equiv (M, \gamma M)$, wherein M is the critical value of the Marangoni number for a given γ varying between $-\infty$ and $+\infty$. In the limit of $\gamma \to 0+$, $M = 48$ (point 1) while $M^{(A)}$ varies according to $M^{(A)} = \gamma M$. Note the existence of a narrow range corresponding to small positive γ where the critical value of the Marangoni number M remains constant, $M = 48$. As stressed above, the critical Marangoni number M decreases to zero with $\gamma \to +\infty$, while $M^{(A)}$ tends to a constant value, $M^{(A)} \to 13{\cdot}5$ (point 2) for the chosen set of the parameters. For $\gamma \to 0-$ (equivalent to $a \to -\infty$) there is a strong stabilization of the layer owing to the heating at the free surface and therefore $M \to -\infty$ (point 3). In the limit of $\gamma \to -\infty$ $(a \to 0-)$ we obtain a result identical to that of $\gamma \to +\infty$. The critical wavenumber increases when γ varies between 0 and $-\infty$.

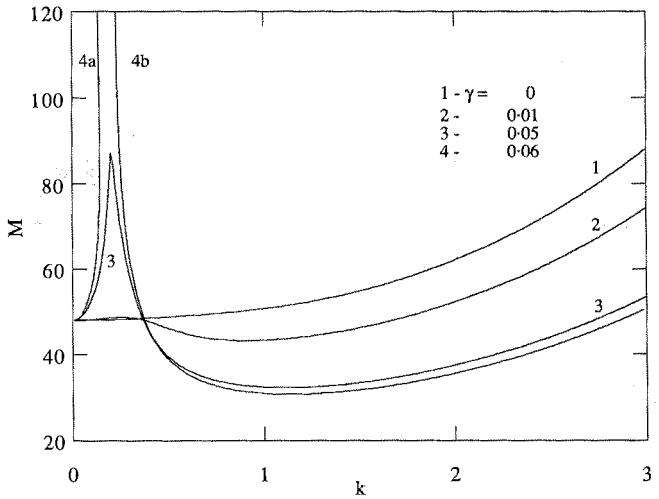

Figure 1. The neutral curves displaying the critical value of the Marangoni number, M, as a function of the dimensionless wavenumber, k, for $P = 6{\cdot}7, L^{-1} = 101, B = 0$ and various values of γ: $1 - \gamma = 0, 2 - \gamma = 0{\cdot}01, 3 - \gamma = 0{\cdot}05$, 4a and 4b – the longwave and the shortwave branches of the neutral curve for $\gamma = 0{\cdot}06$, respectively. With a further increase of γ the longwave branch of $M(k)$ is pushed closer to the line of $k = 0$ and the critical value of the Marangoni number decreases. Stability (instability) domains are located below (above) the neutral curves shown here.

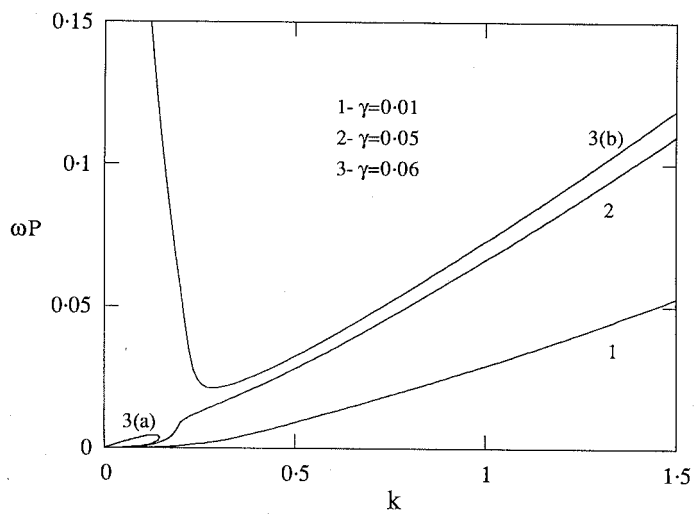

Figure 2. The frequency of the neutral oscillations, ω, as a function of the dimensionless wavenumber. k, for $P = 6{\cdot}7, L^{-1} = 101, B = 0$ and various values of γ: $1 - \gamma = 0{\cdot}01, 2 - \gamma = 0{\cdot}05$, 3(a) and 3(b) correspond to the longwave and the shortwave branches of the neutral curve for $\gamma = 0{\cdot}06$, respectively. Note that for $\gamma = 0$ the instablity is stationary and $\omega = 0$.

4. Weakly nonlinear analysis

In this section we study the nonlinear evolution of the considered system for small values of γ when the instability is longwave. We use the technique of asymptotic expansions to derive a nonlinear evolution equation describing the spatio-temporal behavior of the system. The asymptotic method employed here is based on the fact that, according to the linear stability

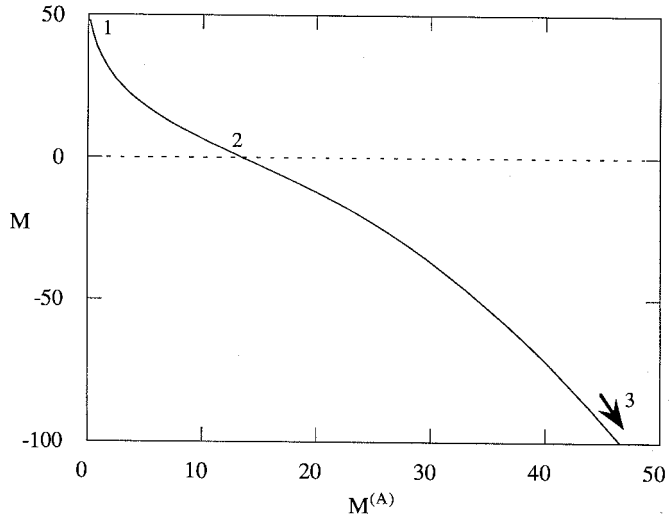

Figure 3. Critical Marangoni number M-tangential Marangoni number $M^{(A)}$ curve for $-\infty < \gamma < \infty$ obtained from the linear analysis. Point 1 corresponds to $\gamma = 0+, 2$ to $\gamma = \pm\infty$ and 3 to $\gamma = 0-$. The domain of stability (instability) is located below (above) the curve shown. Note that the onset of instability is independent of the direction of the tangential gradients (*i.e.* is invariant with respect to A $\rightarrow -A$) and therefore there exists an additional branch of the curve symmetric with respect to the M-axis.

analysis of the system, the characteristic dimensions of the convective cells near the critical threshold are much larger than the thickness of the layer when γ is small. Therefore, it is possible to 'separate' the spatial variables of the problem by their appropriate scalings and then to reduce its dimension. The method was used earlier in different contexts [13–17] and others in the scalar version when only one passive scalar (temperature) is present and in [18] in its vectorial extension for two passive scalars (temperature and concentration) appearing in the equations.

The set of dimensionless governing equations in terms of the streamfunction $\psi(x, z, t)$ is given by

$$\begin{aligned} &\nabla^2\psi_t + (\psi_z\nabla^2\psi_x - \psi_x\nabla^2\psi_z) - P\nabla^4\psi = 0, \\ &T_t + \gamma\psi_z + \psi_x + \psi_z T_x - \psi_x T_z - \nabla^2 T = 0, \\ &L^{-1}C_t + \psi_z + L^{-1}(\psi_z C_x - \psi_x C_z) - \nabla^2 C = 0. \end{aligned} \tag{12}$$

The functions $T(x, z, t)$ and $C(x, z, t)$ constitute the deviations of temperature and concentration from their equilibrium values (6). Here subscripts denote the derivatives with respect to the corresponding variables, $\nabla^2 = \partial^2/\partial x^2 + \partial^2/\partial z^2$, and $\nabla^4 = (\nabla^2)^2$. The boundary conditions follow from Equations (10)

$$\begin{aligned} &\psi = \psi_z = T_z = C_z = 0 \quad \text{at } z = 0, \\ &\psi = C_z = 0, \qquad T_z = -BT, \qquad \psi_{zz} = -M(T_x - L^{-1}\gamma C_x) \quad \text{at } z = 1. \end{aligned} \tag{13}$$

The Marangoni number near the critical point is represented in the form

$$M = M_0(1 + m\epsilon), \tag{14}$$

where M_0 is the value of the Marangoni number at the threshold of instability, ϵ serving, therefore, as a measure of supercriticality and m is its value in units of M_0. Let us introduce the rescaled spatial and temporal variables by

$$\xi = \sqrt{\epsilon}\, x, \qquad \eta = z, \qquad \tau = \epsilon^2 t, \tag{15}$$

where ϵ is a small parameter. The Biot number B is assumed to be small

$$B = \epsilon^2 \beta,$$

wherein $\beta \sim O(1)$ is the rescaled Biot number of the system. Finally, the ratio between the tangential and the normal temperature gradients is assumed to be small

$$\gamma = \sqrt{\epsilon}\,\tilde{\gamma} \tag{16}$$

and $\tilde{\gamma} \sim O(1)$ is the rescaled value of the parameter γ.

The appropriate scaling for the functions ψ, T and C is

$$\psi(x,z,t) = \sqrt{\epsilon}\,\tilde{\psi}(\xi,\eta,\tau), \qquad T(x,z,t) = \tilde{T}(\xi,\eta,\tau),$$
$$C(x,z,t) = \tilde{C}(\xi,\eta,\tau). \tag{17}$$

We solve the system (12–17) using the method of asymptotic expansions. The unknowns are represented as a series in powers of ϵ (tildes are omitted)

$$\{\psi, T, C\} = \{\psi^{(0)}, T^{(0)}, C^{(0)}\} + \epsilon\{\psi^{(1)}, T^{(1)}, C^{(1)}\} + \epsilon^2\{\psi^{(2)}, T^{(2)}, C^{(2)}\} + \cdots. \tag{18}$$

At zeroth order of approximation of Equations (12–18) we obtain

$$T^{(0)} = F(\xi,\tau), \qquad C^{(0)} = G(\xi,\tau), \qquad \psi^{(0)} = \tfrac{1}{4} M_0 (F_\xi - L^{-1}\gamma G_\xi)\eta^2(1-\eta), \tag{19}$$

where F and G are functions of ξ and τ yet unknown and to be determined later.

The solvability condition at zeroth order of approximation can be written as

$$\begin{pmatrix} 1 - M_0/48 & L^{-1}\gamma M_0/48 \\ 0 & 1 \end{pmatrix} \frac{\partial^2}{\partial \xi^2} \begin{pmatrix} F \\ G \end{pmatrix} = \begin{pmatrix} 0 \\ 0 \end{pmatrix}. \tag{20}$$

Equation (20) has a solution if and only if $M_0 = 48$ and the eigenvector corresponding to the zero eigenvalue is

$$\mathbf{q} = \begin{pmatrix} 1 \\ 0 \end{pmatrix}.$$

Also, the solution for Equation (20) is given by

$$\begin{pmatrix} F \\ G \end{pmatrix} = \phi \mathbf{q}, \tag{21}$$

where ϕ is a function of ξ and τ. It follows from Equation (21) that $G \equiv 0$; therefore $C^{(0)} \equiv 0$.

At first order in ϵ Equations (12–18) yield

$$T^{(1)} = Q(\xi,\tau) + \mathcal{F}(\eta;F), \qquad C^{(1)} = Y(\xi,\tau) + 4\gamma L^{-1}\eta^3(1-3\eta/4)F_\xi, \tag{22}$$

where $\mathcal{F}(\eta;F)$ is a polynomial in η with coefficients containing derivatives of F with respect to ξ and Q, Y are functions of ξ, τ, yet unknown. The function $\psi^{(1)}$ is not given here due to its length. The solvability condition at first order is

$$\frac{\partial}{\partial\tau}\begin{pmatrix} F \\ 0 \end{pmatrix} + \frac{\partial}{\partial\xi}\int_0^1 \begin{pmatrix} \psi^{(0)}T_\eta^{(1)} \\ \psi^{(0)}C_\eta^{(1)} \end{pmatrix} \mathrm{d}\eta + \int_0^1 \begin{pmatrix} \psi_\xi^{(1)} \\ 0 \end{pmatrix} \mathrm{d}\eta$$

$$+\beta\begin{pmatrix} F \\ 0 \end{pmatrix} - \frac{\partial^2}{\partial\xi^2}\int_0^1 \begin{pmatrix} T^{(1)} \\ LC^{(1)} \end{pmatrix} \mathrm{d}\eta = \begin{pmatrix} 0 \\ 0 \end{pmatrix}. \tag{23}$$

Substituting Equations (22) in Equation (23) we obtain

$$A\begin{pmatrix} Q \\ Y \end{pmatrix} = \mathbf{r}, \tag{24}$$

where A is the matrix of Equation (20) with $M_0 = 48$ and $\mathbf{r}$ is a vector with the components expressed via F. The nonhomogeneous Equation (24) is solvable if and only if

$$\mathbf{r}\cdot\mathbf{s} = 0, \tag{25}$$

where

$$\mathbf{s} = (-L\gamma^{-1}, 1)$$

is the eigenvector corresponding to the zero eigenvalue of the transposed matrix A^T.

Direct calculation of Equation (25) yields the evolution equation

$$F_\tau + \beta F + mF_{\xi\xi} - \tfrac{96}{35}\gamma(1-L^{-2})F_\xi F_{\xi\xi} - \tfrac{144}{35}F_\xi^2 F_{\xi\xi} +$$

$$+\left(\frac{13}{10}+\frac{2}{5P}\right)(F_\xi F_{\xi\xi})_\xi + \tfrac{3}{5}\gamma(1-L^{-1})F_{\xi\xi\xi} + \tfrac{1}{15}F_{\xi\xi\xi\xi} = 0. \tag{26}$$

This is our key result which in what follows will provide us with the details of the weakly nonlinear behavior of the system. The second component of Equation (24) yields an equation for the unknown function Y

$$Y_{\xi\xi} = -\tfrac{2}{35}(7F_{\xi\xi\xi} + 48L^{-1}F_\xi F_{\xi\xi}). \tag{27}$$

Using scaling

$$F = \sqrt{\tfrac{7}{432}}f \quad \text{and} \quad \xi = \frac{1}{15^{1/4}}\zeta,$$

we obtain

$$f_\tau + \alpha_2 f_{\zeta\zeta} + f_{\zeta\zeta\zeta\zeta} + \beta f + \alpha_3 f_{\zeta\zeta\zeta} - \alpha_1 f_\zeta f_{\zeta\zeta} + \alpha_4(f_\zeta f_{\zeta\zeta})_\zeta - f_\zeta^2 f_{\zeta\zeta} = 0, \tag{28}$$

where

$$\alpha_1 = \frac{8\gamma(1-L^{-2})15^{1/4}}{\sqrt{35}}, \qquad \alpha_2 = \sqrt{15}m,$$

$$\alpha_3 = \frac{3\gamma(1-L^{-1})15^{3/4}}{5}, \qquad \alpha_4 = \sqrt{7/48}\,(13/2 + 2/P).$$

The linear part of Equation (28) consists of the instability term, $\alpha_2 f_{\zeta\zeta}$ induced by a *positive* deviation of the *normal* Marangoni number from its critical value $M_0 = 48$; the stabilizing term $f_{\zeta\zeta\zeta\zeta}$ arising from the dissipative effects such as fluid viscosity, thermal conductivity and solute diffusivity; the damping term βf due to the heat flux from the fluid to the environment at the free surface and the linear dispersive term $\alpha_3 f_{\zeta\zeta\zeta}$ arising from the presence of the tangential temperature and concentration gradients and the difference between the rates of transfer by thermal and solute diffusivities. The nonlinear part of Equation (28) contains, respectively, the quadratic 'diffusive' and 'dispersive' terms and the stabilizing cubic 'diffusive' term known to impose an upper bound for the amplitude of the emerging pattern.

When the right–left symmetry of the problem is restored, *i.e.* $\gamma(L^{-1}-1) = 0$, Equation (28) reduces to the evolution equations derived in [14] (if $\alpha_1 = \alpha_3 = \alpha_4 = 0$) in the context of the Rayleigh instability, and in [13, 15] (if $\alpha_1 = \alpha_3 = 0$) for the Rayleigh and Marangoni instabilities, respectively.

Due to the loss of the left–right symmetry caused by both the action of the tangential temperature and concentration gradients and the departure of the inverse Lewis number from unity, the evolution Equation (28) is not invariant under the transformation $\zeta \to -\zeta$. The 'non-symmetric' terms are associated with the coefficients α_1 and α_3. It is clear that the symmetry is restored when $\gamma(L^{-1} - 1) = 0$. Also, due to large characteristic values of the inverse Lewis number, L^{-1}, ($L^{-1} = 101$ for a water-salt solution) the relative magnitude of the linear dispersive term, α_3, is much smaller than that of the term α_1.

We now turn to a study of stability properties of the trivial solution, $f = 0$, for Equation (28) and to its bifurcation analysis in the case of a nonzero Biot number, $\beta \neq 0$. The linearized version of Equation (28) is

$$f_t + \alpha_2 f_{\zeta\zeta} + f_{\zeta\zeta\zeta\zeta} + \beta f + \alpha_3 f_{\zeta\zeta\zeta} = 0. \tag{29}$$

Substituting a normal perturbation in the form $f = \exp(\lambda t + ik\zeta)$ in Equation (28) we obtain the dispersion relation for the growth rate λ

$$\lambda = -\beta + \alpha_2 k^2 - k^4 + ik^3\alpha_3. \tag{30}$$

The real part of the λ determines the stability ($\mathrm{Re}(\lambda) < 0$) or instability ($\mathrm{Re}(\lambda) > 0$) domains of the zero solution. A nonzero imaginary part of λ, $\mathrm{Im}(\lambda) = k^3\alpha_3$ shows that the instability is oscillatory. The threshold of instability is found from the condition $\mathrm{Re}(\lambda) = 0$

$$\alpha_2 = \frac{\beta}{k^2} + k^2. \tag{31}$$

The minimal value of the parameter α_2 is attained at the point

$$\alpha_{2c} = 2\sqrt{\beta}, \qquad k_c = \beta^{1/4}. \tag{32}$$

It follows from our linear stability analysis that in the case of a zero Biot number, $B = 0$, the instability is longwave, *i.e.* $k_c = 0$. In contrast with this, for nonzero B the instability is to the perturbations with a nonzero wavenumber, *i.e.* $k_c \neq 0$. This feature is fairly common for problems related to thermal convection. The neutral curves as obtained from our linear stability analysis for various γ and *small* $B \neq 0$, if they were displayed, tend to infinity as $k \to 0$, decrease with k, reach a minimum point and then approach the neutral curve corresponding to $B = 0$ at larger k. That minimum corresponding to the onset of instability is reached at $k = k_c = \beta^{1/4}$, Equation (32). Note that $\beta = 0$ yields $k_c = 0$, as stated above. The value of α_{2c} given by Equation (32) corresponds to the location of the instability threshold *above* the critical value of $M_0 = 48$ held for $\beta = 0$. As follows from the analysis presented in the text containing Equations (29)–(32) there is *no* instability in the considered regime for $\alpha_2 < \alpha_{2c}$. Note that α_2 is related to the value m, Equation (28), being the value of supercriticality, *i.e.* the distance between the actual Marangoni number and its critical value $M_0 = 48$, *cf.* Equation (14).

Going into the frame of reference moving with the speed $c, \zeta^* = \zeta - c\tau, t = \tau$, expanding the variables in the vicinity of the critical point [14, 15]

$$t = \delta^2 t^*, \qquad \alpha_2 = \alpha_{2c} + \delta^2 + \cdots,$$
$$c = c_0 + c_1\delta^2 + \cdots, \qquad f = \delta f_1 + \delta^2 f_2 + \delta^3 f_3 + \cdots \tag{33}$$

and introducing these into Equation (28), we obtain at first order of expansion in δ (δ is a small parameter, being the distance between the actual value of α_2 and its critical value given by Equation (32)) up to a phase shift in ζ^*

$$c_0 = \alpha_3\beta^{1/2}, \qquad f_1 = A(t^*)\cos(\beta^{1/4}\zeta^*),$$

where $A(t^*)$ is a function of t^*. Continuing the expansion up to the terms of third order in δ, we obtain the Landau equation for the amplitude function $A(t^*)$

$$\frac{\mathrm{d}A}{\mathrm{d}t^*} = \sqrt{\beta}\,A - \kappa A^3, \tag{34}$$

where the Landau constant κ is

$$\kappa = \frac{\beta(-2\alpha_1^2 + 9\sqrt{\beta} + 4\alpha_3^2 - 4\alpha_1\alpha_3\alpha_4 + 4\sqrt{\beta}\,\alpha_4^2)}{36\sqrt{\beta} + 16\alpha_3^2} \tag{35}$$

If the sign of κ is positive, the bifurcation from the quiescent state to a motion is supercritical. However, a negative sign of κ suggests that the bifurcation is subcritical. In the limiting case of the pure Marangoni instability, $\gamma = 0$, the Landau constant κ is positive and the bifurcation is supercritical. This result coincides with that of [15]. Evaluation of the Landau constant κ shows that for large values of the inverse Lewis number L^{-1} it changes its sign from positive to negative at very small values of γ. For instance, if $L^{-1} = 101, P = 6{\cdot}7$ (water-salt solution), κ changes its sign at $\gamma \approx 4{\cdot}671 \times 10^{-5}$. Thus the primary bifurcation is subcritical for vanishingly small tangential gradients.

5. Traveling-wave solutions

In order to explore traveling wave solutions for Equation (28) with $\beta = 0$ we introduce $f = f(Z), Z = \zeta - vt$, where v is the wave speed. Integrating it with respect to z and looking for localized or solitary waves that satisfy the conditions

$$f \to f_0, \qquad f' \to 0, \qquad f'' \to 0, \qquad f''' \to 0 \quad \text{at } Z \to \pm\infty,$$

we obtain an o.d.e.

$$f''' + \alpha_3 f'' + \alpha_2 f' + v(f_0 - f) - \frac{\alpha_1}{2} f'^2 + \alpha_4 f' f'' - \tfrac{1}{3} f'^3 = 0, \tag{36}$$

where primes denote differentiation with respect to Z.

We are now interested in elucidating the behavior of the solutions at the leading and trailing edges of the pulse. To achieve that we represent Equation (36) in the form of the dynamical system in terms of $u_1 \equiv f - f_0, u_2 \equiv f', u_3 \equiv f''$

$$u_1' = u_2, \qquad u_2' = u_3, \qquad u_3' = v u_1 - \alpha_2 u_2 - a_3 u_3 - \alpha_4 u_2 u_3 + \tfrac{1}{2}\alpha_1 u_2^2 + \tfrac{1}{3} u_2^3. \tag{37}$$

Linearizing this system around its stationary point

$$\tilde{u}^{(0)} \equiv u_1 = u_2 = u_3 = 0$$

and looking for the asymptotic behavior of the homoclinic orbit that start and terminate at $\tilde{u}^{(0)}$, we obtain the characteristic equation

$$s^3 + \alpha_3 s^2 + \alpha_2 s - v = 0. \tag{38}$$

Let us begin with the simplest supercritical case of $\alpha_2 > 0$ with $\alpha_3 = 0$. In this case Equation (38) reduces to $s^3 + \alpha_2 s - v = 0$ and the latter has always one real root $s = s_1$ and a pair of complex conjugate roots $s_{2,3} = -s_1/2 \pm i\tilde{s}$. We assume that the wave speed v is positive. Then $s_1 > 0$ and $\mathrm{Re}(s_{2,3}) < 0$. Therefore the corresponding eigenfunctions are

$$f_1 \sim \exp(s_1 Z), \qquad f_2 \sim \exp(-\tfrac{1}{2} s_1 Z) \sin(\tilde{s} Z + \varphi), \tag{39}$$

where φ is a phase shift. Hence, the unstable manifold at $\tilde{u}^{(0)}$ is one-dimensional and the stable manifold at $\tilde{u}^{(0)}$ is two-dimensional. According to Equations (39) the solution is monotonic at $Z \to -\infty$ (at the trailing edge of the pulse) and oscillating with decaying amplitude at $Z \to +\infty$ (at the leading edge of the pulse). In the case of negative v the stable (unstable) manifold is two-dimensional (one-dimensional) and thus for $Z \to -\infty$ ($Z \to +\infty$) the solution has damped oscillations (a monotonic tail). Due to the change in the direction of the wave propagation the conclusion related to the solution behavior for $v > 0$ remains true in the case of $v < 0$ as well.

Turning back to the case of $\alpha_3 \neq 0$, we notice that under the transformation $s \to s + \alpha_3/3$ Equation (44) reduces to

$$s^3 + ps + q = 0$$

with $p = \alpha_2 - \alpha_3^2/3, q = -v - \alpha_2\alpha_3/3 - 2\alpha_3^3/27$. The analysis performed above can be repeated and the conclusions drawn about the asymptotic behavior of the solutions of Equation (28) remain the same if $p > 0$, *i.e.* $\alpha_2 > \alpha_3^2/3$.

Leaving a direct integration of Equation (36) to find solitary traveling-wave patterns emerging in the system under consideration beyond the scope of the paper, we proceed to the numerical study of the full evolution Equation (28) to determine the relevant solutions of a wavetrain type.

6. Numerical results

We solve numerically Equation (28) in the domain $0 \leqslant \zeta \leqslant \Delta$ with periodic boundary conditions with the initial condition.

$$f_0 \equiv f(\zeta, \tau = 0) = 0{\cdot}0001 \sin(2\pi\zeta/\Delta). \tag{40}$$

The size of the periodic domain Δ is chosen to be large enough to include the fastest wavelength. In this study we carry out our computations for the case of thermally insulated boundaries, $\beta = 0$ and for $P = 6{\cdot}7, L^{-1} = 101, \alpha_2 = 0{\cdot}01$ (corresponding to $m = 0{\cdot}0258$) while γ varies in the range between 0 and 10^{-4} and $\Delta = 32\pi$. When the solution for Equation (28), $f(\zeta, \tau)$, is found, the streamfunction, temperature and concentration perturbations fields are, respectively, given to their leading order by the rescaled Equations (19) and (22)

$$\begin{aligned} &\psi^{(0)} = (7/3)^{1/2} 15^{1/4} f_\zeta \eta^2 (1-\eta), \qquad T^{(0)} = (7/432)^{1/2} f, \\ &C^{(1)} = \hat{Y}(\zeta, \tau) + \gamma L^{-1} (7/27)^{1/2} 15^{1/4} f_\zeta \eta^3 (1 - 3\eta/4), \end{aligned} \tag{41}$$

where we obtained $\hat{Y}(\zeta, \tau)$ by numerical integration of the rescaled Equation (27) using periodicity conditions in the ζ-direction and the conservation of solute concentration.

It is found to be useful to characterize the solutions of Equation (28) by the integral value

$$E = \int_0^\Delta [u(x)]^2 \, \mathrm{d}x,$$

being the square of the L_2-norm of the function $u(x)$ in $[0, \Delta]$. E expresses, therefore, the magnitude of the solution.

Equation (28) is found to lead to travelling-wave solutions resulting from the evolution of the initial data. Equation (40). Numerical calculations are stopped when the temporal variation of E becomes small. $|\mathrm{d}E/\mathrm{d}t| \leqslant 10^{-6}$.

In the case of $\gamma = 0$ corresponding to the symmetric configuration with no lateral temperature and concentration gradients the evolution of the initial condition leads to the emergence of a steady solution. The introduction of a nonzero value of γ results in the loss of the left–right symmetry and the pattern propagates along the layer from the right to the left. The direction of wave propagation is consistent with the one already predicted in the linear stability analysis, Equations (11): for $\gamma > 0$ and $L^{-1} > 1$ the value ω is positive, *i.e.* the wave propagates to the left. Evolution of the initial data (40) leads ultimately to traveling-wave solutions which are found numerically to be stable under small perturbations. These waves have an oscillatory leading edge and a monotonic tail similarly to the localized waves considered in Section 5. The wave speed increases with γ. In the range $0 < \gamma < 2 \times 10^{-5}$ both the amplitude of the solution $f(\zeta, \tau)$ and the value of the 'energy' E increase with γ. In the vicinity of $\gamma \approx 2 \times 10^{-5}$ the

amplitude of the solution starts to decrease with γ and E decreases abruptly. From now on the solution develops a deep trough and a plateau-like domain with a small hump (or humps). The trough part of the wave becomes deeper and narrower, while the plateau becomes wider with increase of γ. The value of E decreases with γ. It is also found that for γ slightly higher than 10^{-4} stable multi-humped travelling waves result from the time evolution of the initial data. Equation (40). Figures 4–6 show the instantaneous fields of streamlines, temperature and solute concentration perturbations for various values of γ. The fields of temperature perturbations are independent of the normal co-ordinate η and are represented by the solution of Equation (28), $f(\zeta, \tau)$. The streamlines and concentration fields are calculated by means of Equation (41). We have drawn the contour plots using the grey scale with black and white corresponding to the minimal and maximal values of the field, respectively. The field of the solute concentration perturbations is found to have a very weak dependence on η and is represented by its tangential cross-section. Note that the feature of a weak η-dependence of the solute concentration is not general and is owing to the large value of the inverse Lewis number L^{-1} which is true in most cases of interest. All patterns shown in these figures propagate from the right to the left. The flow fields shown have an asymmetric cellular structure of counter-rotating vortices. With increase of γ the overall area of the convective cells contract, while the area of the quiescent domain expands. Small secondary cells are found in the case of a higher γ, see Figure 4c. As common for the Marangoni flows induced by a vertical temperature gradient (*cf.* [15]) the ζ-component of the flow field changes its direction at $\eta = 2/3$. This can be easily seen from Equation (41). Similar to the case of the pure Marangoni instability $(\gamma = 0)$ the counter-rotating convective cells are contained between the locations of the minimal and maximal temperature perturbations. It follows from Equations (41) that ascending (descending) flows correspond to the locally hottest (coldest) spots at the film interface.

Figure 7 displays the variation of E as a function of γ as found from the numerical solution of Equation (28). As said above, the transition of the solution's topology from a sinusoidal-like shape to a localized pulse is associated with the abrupt drop of E. This fact suggests that at γ corresponding to that steep decrease of E sinusoidal wave solutions lose their stability to localized pulses. Indeed, a sinusoidal wave emerges as a transient; however, it does not survive during the nonlinear stage of the evolution.

7. Discussion

The issue which has to be addressed now is the relevance of the problem considered here for laboratory experiments. The main point is the emergence of an advective horizontal flow induced by both temperature and concentration gradients when the system is studied in the ground-based facility. This flow, however, is not encountered in zero-gravity conditions in space.

Let us now estimate the conditions under which it is correct to neglect the advective flow even in ground-based laboratory conditions. The magnitude of the advective component of heat/mass transfer is represented in Equations (1) by the terms $|\mathbf{v} \cdot \nabla T|$ and $|\mathbf{v} \cdot \nabla C|$ respectively, while that of the molecular phenomena (thermal conduction and mass diffusion) by $\chi \nabla^2 T$ and $D \nabla^2 C$, respectively.

The impact of the base advective flow can be neglected with respect to that of the transfer due to the corresponding molecular mechanisms if

$$|\mathbf{v} \cdot \nabla T| \ll \chi \nabla^2 T \quad \text{and} \quad |\mathbf{v} \cdot \nabla C| \ll D \nabla^2 C. \tag{42}$$

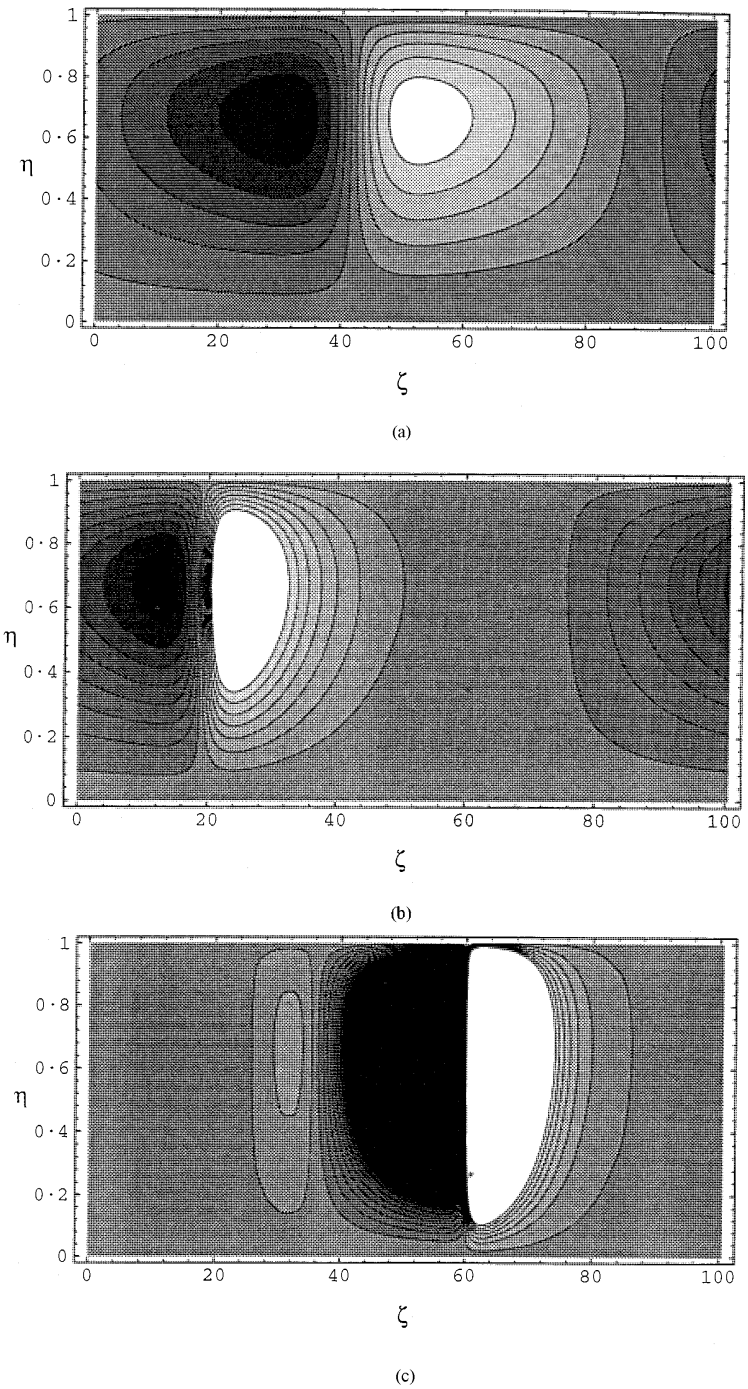

Figure 4. Streamline pattern as obtained from the weakly nonlinear theory, Equations (41), for $\beta = 0, P = 6{\cdot}7, L^{-1} = 101, \alpha_2 = 0{\cdot}01, \Delta = 32\pi$ and for (a) $\gamma = 2{\cdot}5 \times 10^{-6}$, (*b*) $\gamma = 3 \times 10^{-5}$, (c) $\gamma = 7 \times 10^{-5}$. The patterns displayed here propagate from the right to the left as a traveling wave. A pair of secondary convective cells (one of them is not shown due to its extremely slow circulation) associated with the local extrema of the function f displayed in Figure 6 (curve 3) emerge in the system.

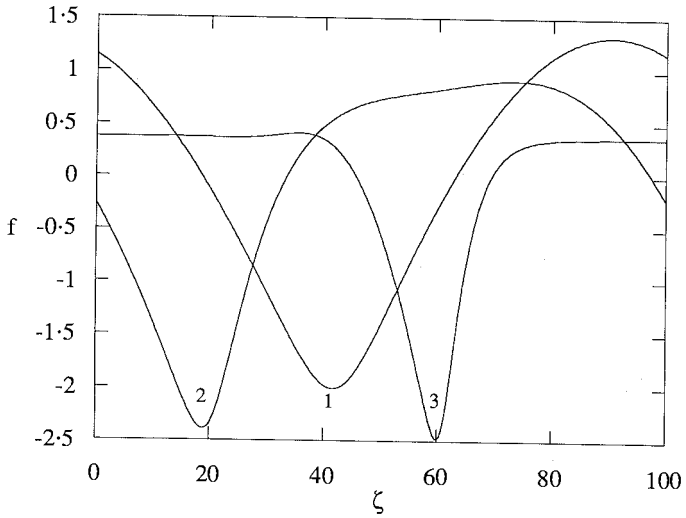

Figure 5. The fields of thermal perturbations, as obtained from the weakly nonlinear theory, Equations (41), for $\beta = 0$, $P = 6{\cdot}7$, $L^{-1} = 101$, $\alpha_2 = 0{\cdot}01$, $\Delta = 32\pi$ and (a) $\gamma = 2{\cdot}5 \times 10^{-6}$, (b) $\gamma = 3 \times 10^{-5}$, (c) $\gamma = 7 \times 10^{-5}$. Note that the temperature perturbations fields are η-independent and represented therefore by their longitudinal cross-section. The patterns displayed here propagate from the right to the left as a traveling wave.

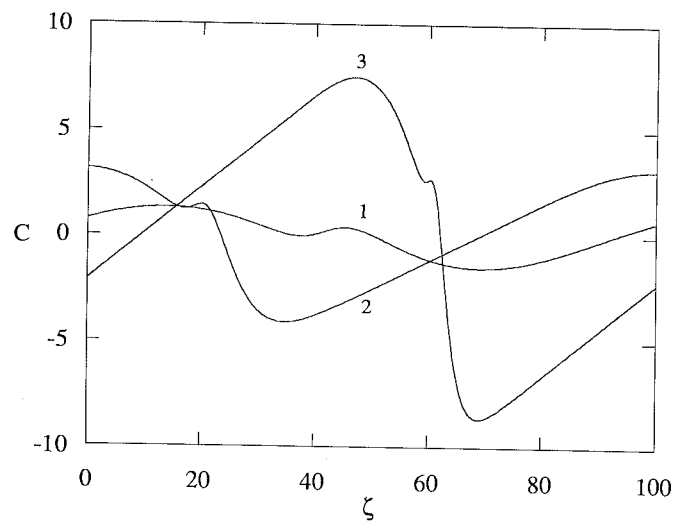

Figure 6. The fields of solute concentration perturbations, as obtained from the weakly nonlinear theory, Equations (41), for $\beta = 0$, $P = 6{\cdot}7$, $L^{-1} = 101$, $\alpha_2 = 0{\cdot}01$, $\Delta = 32\pi$ and for (a) $\gamma = 2{\cdot}5 \times 10^{-6}$, (b) $\gamma = 3 \times 10^{-5}$, (c) $\gamma = 7 \times 10^{-5}$, all calculated at $\eta = \frac{1}{2}$. The patterns displayed here propagate from the right to the left as a traveling wave.

We will employ these inequalities to evaluate the domain of validity of the considered model.

Using the characteristic velocities associated with the thermo-gravitational and soluto-gravitational effects, $g\beta_t Ah^3/\nu$ and $g\beta_c A_c h^3/\nu$, respectively, where g is the gravitational acceleration, A and A_c are tangential temperature and concentration gradients, and β_t and β_c

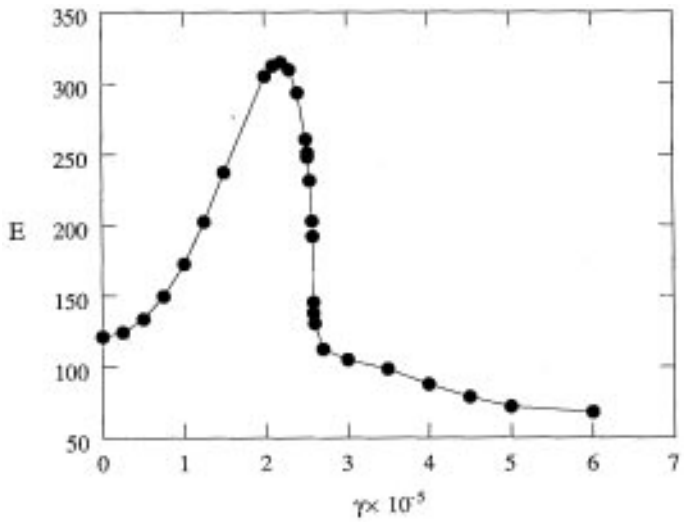

Figure 7. 'Energy' E of traveling wave solutions for Equation (28) as a function of γ with $\alpha_2 = 0{\cdot}01, \beta = 0, L^{-1} = 101, P = 6{\cdot}7$ and the initial condition, Equation (40).

are, respectively, coefficients of thermal and solutal expansion of the fluid we obtain, using Equations (42), the following estimates for the thermal and solutal Rayleigh numbers

$$Ra_t = \frac{g\beta_t A h^4}{\nu\chi} \ll 1, \qquad Ra_c = \frac{g\beta_c A_c h^4}{\nu D} \ll 1. \tag{43}$$

Introducing $A = \Delta T_{||}/d$, $A_c = \Delta C_{||}/d$, where $\Delta T_{||}, \Delta C_{||}$ are the temperature and concentration variations along the layer, respectively, and d its length, into Equations (43) and solving them for h leads to

$$h \ll \min\left[\left(\frac{\nu\chi}{g\beta_t\Delta T_{||}}\cdot\frac{h}{d}\right)^{1/3}, \left(\frac{\nu D}{g\beta_c\Delta C_{||}}\cdot\frac{h}{d}\right)^{1/3}\right]. \tag{44}$$

The tangential temperature and concentration variations should be small enough to ensure the validity of the Boussinesq approximation $\beta_t\Delta T_{||} \ll 1, \beta_c\Delta C_{||} \ll 1$. For instance, let us take $\beta_c\Delta C_{||} \sim 0{\cdot}01$ for a layer of the aspect ratio $h/d = 10^{-2}$. Then using $\beta_c = 0{\cdot}005$ (% solute mass fraction)$^{-1}$ we have $\Delta C_{||} = 2\%$ solute mass fraction. $\Delta T_{||}$ will be calculated from the equilibrium condition, Equation (6), $\sigma_c\Delta C_{||} = \sigma_t\Delta T_{||}, \Delta T_{||} = 4{\cdot}9\,\mathrm{K}$. The value of $\beta_t\Delta T_{||}$ for the case considered, $\beta_t = 2{\cdot}0 \times 10^{-4}\,\mathrm{K}^{-1}$, is then of order of magnitude of 10^{-3}, *i.e.* small to validate the use of the Boussinesq approximation. We can now calculate the normal temperature variation $\Delta T_\perp$ via

$$\Delta T_\perp = \frac{\Delta T_{||}}{\gamma}\frac{h}{d},$$

which yields $\Delta T_\perp = 4{\cdot}9 \times 10^{-2}/\gamma\,\mathrm{K}$. We obtain then from Equation (44) the estimate for the layer thickness, $h \ll 0{\cdot}011\,\mathrm{cm}$.

Table 1. Material properties for dilute salt-water mixtures at 20°C. Compiled from [19]. For dilute salt-water mixtures only σ_c is found to be relatively sensitive with respect to solute concentration variations.

ρ (g/cm^3)	1·003
μ (g/cm · s)	0·0102
ν (cm^2/s)	0·01015
D (cm^2/s)	$1{\cdot}5 \times 10^{-5}$
χ (cm^2/s)	0·0015
σ (dyne/cm)	73·07
σ_t (dyne/cm · K)	0·15
σ_c (dyne/cm · % solute mass fraction)	0·367
P	6·7
L^{-1}	101

On the other hand, the 'normal' Marangoni number M defined in Section 2 and rewritten as

$$M = \frac{\sigma_t \Delta T_{||} h}{\gamma \nu \rho \chi} \cdot \frac{h}{d}$$

exceeds the maximal critical value of $M_0 = 48$ for a chosen value of $h = 0{\cdot}0025$ cm when $\gamma < 0{\cdot}025$. Let us reiterate that these values of γ correspond to the coupled double-diffusive Marangoni instability dealt with in the present work when the buoyancy-driven effect can be justifiably neglected. This 'allowed', range of γ and also the 'allowed' thickness of the layer can be both extended when we consider the layer of a larger aspect ratio. For example, if the aspect ratio of the layer is $h/d = 10^{-3}$, then $h \ll 0{\cdot}025$ cm, and choosing $h = 0{\cdot}005$ cm yields $\gamma < 0{\cdot}005$.

It is emphasized that reducing the gravity *i.e.* going to the microgravity conditions, say to $10^{-6}g$, allows us to increase the thickness of the layer and the relevant range for the parameter γ, making them 100 times larger than in $1g$.

The study of stability properties of the no-flow equilibrium state undertaken here can be viewed as the first approximation for the investigation of the stability of a weak advective flow giving a rough estimate of the heat-mass transfer processes driven by Marangoni stresses in dilute binary mixtures with temperature and concentration gradients slightly tilted from the vertical direction. The significance of the consideration of slightly tilted temperature and concentration gradients arises from their presence in many laboratory experiments and technological processes as undesirable factors. Our analysis shows a sizeable impact of small tangential temperature and concentraton gradients on the stability properties of the system.

We have studied the onset of instability in a binary liquid layer open to the atmosphere and subjected to simultaneously acting vertical temperature gradient and tangential temperature and solute concentration gradients. A quiescent state of the layer is possible for specially chosen values of the tangential gradients such that the surface tractions, due separately to temperature- and concentration inhomogeneities at the interface, vanish. It is found that for very small tangential gradients the quiescent ground state is unstable and the type of the instability (longwave or shortwave) is determined by the corresponding type of the Marangoni instability due to the presence of the vertical *destabilizing* temperature gradient only. For

larger values of the tangential gradients the instability (double-diffusive instability) is always shortwave. Also, the instability is found to be always oscillatory in the presence of the tangential gradients provided that the inverse Lewis number of the binary liquid is different from unity. Double-diffusive instability persists when no vertical temperature gradient is imposed on the layer or even when the latter is negative, *i.e. stabilizing*. A weakly nonlinear analysis of the case of nearly thermally insulating boundaries yields the nonlinear evolution equation describing the spatio-temporal behavior of the system. It follows from the numerical study of the evolution equation that large convective cells propagate along the layer in the direction depending on the sign of the expression $\gamma(L^{-1} - 1)$.

Acknowledgements

The research was supported by the Fund for the Promotion of Research at the Technion and Japan Technion Society Research Fund. A. Oron thanks Professors S. G. Bankoff, S. H. Davis and D. Halpern for useful discussions and suggestions.

References

1. S.H. Davis, Thermocapillary instabilities. *Ann. Revs. Fluid Mech.* 19 (1987) 403–435 (and references therein).
2. B.A. Vertgeim, On the conditions of appearance of convection in a binary mixture. *Appl. Math. and Mech.* 19 (1955) 747–750.
3. D.A. Nield, The thermohaline Rayleigh–Jeffreys problem. *J. Fluid Mech.* 29 (1967) 545–558.
4. T.G.L. Shirtcliffe, An experimental investigation of thermosolutal convection at marginal stability. *J. Fluid Mech.* 35 (1969) 677–688.
5. J.S. Turner, Double-diffusive phenomena. *Ann. Revs. Fluid Mech.* 6 (1974) 37–56.
6. J.S. Turner, Multicomponent convection. *Ann. Revs. Fluid Mech.* 17 (1985) 11–44.
7. S. Ostrach, Fluid mechanics in crystal growth – The 1982 Freeman Scholar Lecture. *J. Fluids Eng*. 105 (1983) 5–20 (and references therein).
8. C.L. McTaggart, Convection driven by concentration- and temperature-dependent surface tension. *J. Fluid Mech.* 134 (1938) 301–310.
9. K.-L. Ho and H.-C. Chang, On nonlinear doubly-diffusive Marangoni instability. *AIChE J*. 34 (1988) 705–722.
10. T.L. Bergman, Numerical simulation of double-diffusive Marangoni convection. *Phys. Fluids* 29 (1986) 2103–2108.
11. J.R.A. Pearson, On convection cells induced by surface tension. *J. Fluid Mech*. 4 (1958) 489–500.
12. A. Vidal and A. Acrivos, Nature of the neutral state in surface tension driven convection. *Phys. Fluids* 9 (1966) 615–615.
13. C.J. Chapman and M.R.E. Proctor, Nonlinear Rayleigh–Benard convection between poorly conducting boundaries. *J. Fluid Mech*. 66 (1981) 759–782.
14. V.L. Gertsberg and G.I. Sivashinsky, Large cells in nonlinear Rayleigh–Benard convection. *Prog. in Theor. Phys*. 66 (1981) 1219–1229.
15. G.I. Sivashinsky, Large cells in nonlinear Marangoni convection. *Physica* 4D (1982) 227–235.
16. A. Oron and P. Rosenau, Evolution of the coupled Benard–Marangoni convection. *Phys. Rev. A* 39 (1989) 2063–2069.
17. L. Braverman and A. Oron, Weakly nonlinear analysis of the vibrational-convective instability in a fluid layer *Eur. J. Mech. B/Fluids* 13 (1994) 557–572.
18. D. Hefer and L.M. Pismen, Long-scale thermodiffusional convection. *Phys. Fluids* 30 (1987) 2648–2654.
19. *CRC Handbook of Chemistry and Physics*. Cleveland: CRC Press, 58th edn (1978).